Assimilation of Doppler Lidar-derived Planetary Boundary Layer Height Using the Ensemble Kalman Filter During the PECAN Field Campaign

[1]Keming Pan (kmpan@arizona.edu), [2]Andrew Tangborn, [3]Jeffrey J. Anderson, [4]Belay Demoz, [5]Joseph A. Santanello, [6,7]Brian J. Carroll, [1]Avelino F. Arellano
[1]The University of Arizona, [2]Environmental Modeling Center, NCEP/NOAA, [3]Computational and Information System Lab, NSF NCAR, [4]The University of Maryland, Baltimore,
[5]Goddard Space Flight Center, NASA, [6]CIRES, University of Colorado Boulder, [7] NOAA Chemical Sciences Laboratory

THE UNIVERSITY OF ARIZONA

UA SCIENCE
Hydrology & Atmospheric Sciences

Objectives

1. Explore how best to assimilate ground-based data of PBLH (Planetary Boundary Layer Height) into a numerical prediction model (WRF v4.5) using ensemble Kalman filter (DART Manhattan) with multi-physics (three PBL schemes).
2. Investigate the impact of PBL-related data assimilation (DA) on model analyses and short-term forecast.

Measurements, Model & Experiment Set-up

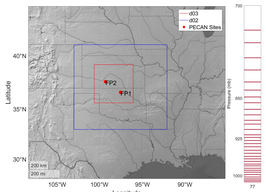


Fig. 1. WRF domain configuration and location of the Plains Elevated Convection at Night (PECAN) sites.

Table 1. Model Configurations

Horizontal Grid Spacing	D01: 10km, D02: 3.3km, D03: 1.1km
Vertical Gridding	77 levels (33 below 700mb, 12 below 950mb)
ICBCs	GFS
Cumulus Scheme	Modified Tiedtke cumulus scheme (D01 only)
Microphysics Scheme	Thompson graupel microphysics scheme
PBL Scheme	MYJ; YSU; MYNN-EDMF
Surface Physics Scheme	Monin-Obukhov-Janjic (MOJ); Monin-Obukhov; MYNN
Land Surface Model	Unified Noah
Radiation Scheme	Rapid Radiative Transfer Mode (longwave and shortwave)

More information regarding the performance of the model with similar setup can be found in Pan et al. (2024) *JAMC*.

Please scan the QR code.

❖ State Update

Analysis algorithm for Ensemble Adjustment Kalman Filter (EAKF) in DART.

State vector $X_n^m, \quad n = 1, \dots, N; \ m = 1, \dots, M$

Inflated prior state vector $\bar{X}_n^m = \lambda_m(X_n^m - \bar{X}^m) + \bar{X}^m, \quad n = 1, \dots, N; \ m = 1, \dots, M$

Observed quantity $y_n = h(\bar{X}_n), \quad n = 1, \dots, N$

Analysis increment $\Delta x_n = \alpha \frac{\sigma_{x,y}}{\sigma_{x,x}} \Delta y_n = \alpha\beta\Delta y_n, \quad n = 1, \dots, N$

$$\lambda = \frac{\left(y_o - \bar{y}_f\right)^2}{\left(\sigma_o^2 + \sigma_f^2\right)}$$

Where m is the number of variables, n is the ensemble size, λ is the inflation, α is the localization (Fig. 4), β is the ensemble-based regression coefficient (Fig. 5), Δy_n is an ensemble of increments, $h(x)$ is the forward operator, here we use the PBL scheme as the PBLH forward operator (See Table 1).

❖ Measurements

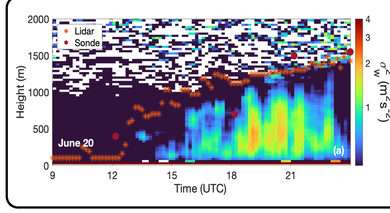


Fig. 2. Doppler lidar-derived PBLH data based on the vertical velocity variance (σ_w^2) profile measured at FP1 on June 20, 2015. The PBLH derived from radiosonde measurement (θ inversion) is included for comparison.

- **DA Analysis and Forecast Cycle.** We start by perturbing the initial conditions (GFS) to generate 30 ensemble members. We then perform PBLH DA using four different strategies (See Table 2&3). Twelve hourly (12-00 UTC) lidar-derived PBLH (see Fig. 2) are assimilated into the WRF model. The ensemble mean analysis is used as initial condition for a 24-hour forecast. See flowchart (Fig. 3) for details.

❖ References

- Tangborn, A., Demoz, B., Carroll, B. J., Santanello, J., & Anderson, J. L. (2021). Assimilation of lidar planetary boundary layer height observations. *Atmospheric Measurement Techniques*, *14*(2), 1099-1110
- Pan, K., Arellano, A. F., Guo, Y., & Demoz, B. (2024). Investigating the Impact of Multiphysics on Modeled Planetary Boundary Layer Height Estimates during the PECAN Field Campaign. *Journal of Applied Meteorology and Climatology*, *63*(11), 1385-1407.

❖ Experiment Set-up for the Test Case (June 20, 2015; LLJ-3)

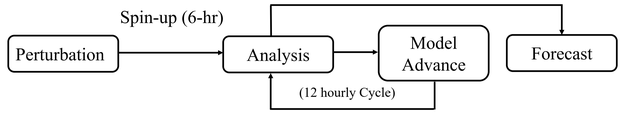


Fig. 3. Flowchart of DA process used in this study (including 6-hr spin-up, 12-hr DA, and 24-hr forecast initialized at 00UTC)

Table 2&3. DA Experiments (top) and DART Assimilation Settings (bottom)

Strategy	Ensemble Size	PBL Scheme	Perturbation and Spin-up
1	30	YSU	Initial spread
2	30	MYJ	Initial spread
3	30	MYNN	Initial spread
4	3×10	MYJ, YSU, MYNN	Initial spread and multi-physics

Pscale	Inflation (λ)	Vertical Localization (α)	Observation Error (σ_o)	Filter
0.25	1.5	Boxcar-Ramp 1km	20%	Rank-Histogram

- **Evaluation Procedure.** A reference run (noDA) is carried out following the exact procedure described in Fig. 3 for comparison. Additionally, two runs incorporating DA using radiosonde-measured T and q profiles (i.e., Sonde T, Sonde T&q) are included. A deterministic forecast is generated at the end of the Analysis-Model Advance cycle (00 UTC), using the mean of 30 ensemble members as the initial condition and a model setup employing MYNN PBL scheme (see Table 1). The state variables (θ, q, U, and V) at the nearest grid point to FP1 (i.e., a single column) are extracted from the DA runs and compared to the noDA run and radiosonde measurements.

Results

❖ Localization (α) & Ensemble-based Regression Coefficient (β)

Fig. 4. Three different types of vertical localization (a-c) tested in this study: Gaspari-Cohn with 1 km cut-off (G-C 1km), G-C with 3 km cut-off, and Boxcar-Ramp with 1km cut-off (B-R 1km). The vertical location of the observation is set to the observed PBLH. The vertical localization used in Tangborn et al. (2021) is shown for comparison. Here three examples of time at 12, 18, and 00 UTC are included. The corresponding horizontal localization (d) is also included for G-C (100 km cut-off) and B-R (50 km cut-off).

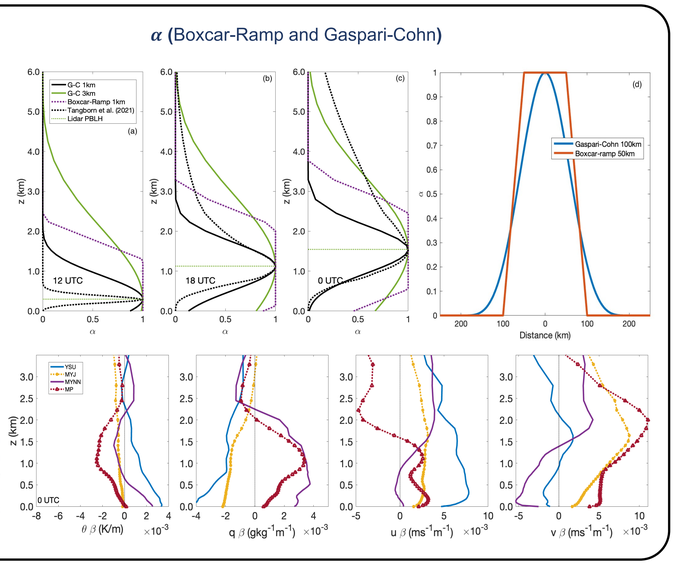


Fig. 5. Regression coefficient β between modeled PBLH and state variables (θ, q, U, and V) for the PBLH DA at 00 UTC (Fig. 8).

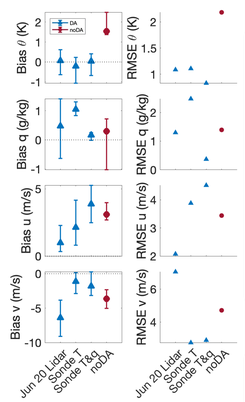


Fig. 10. The bias and RMSE between modeled state variables θ, q, U, and V and measurements for the DA and no-DA runs at 00 UTC shown in Fig. 9. The bias (model-measurement) and RMSE are calculated for the lowest 30 model levels (~below 2.5 km). The error bars denote the median, 25th and 75th percentiles of the bias.

Multi-Physics (MP) vs. Single-Physics

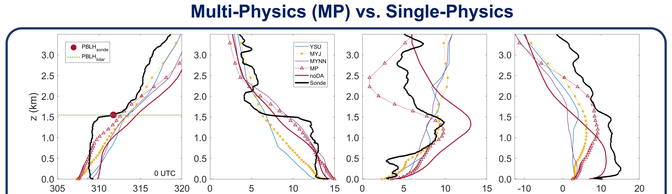


Fig. 8. Comparisons for θ, q, U, and V profiles (FP1) at 00 UTC on June 20, 2015, illustrating the analysis of the PBLH DA using multi-physics (MP, triangle marker) and three single-physics (see Table 2&3). The reference run without DA (noDA, solid red), radiosonde measurements (solid black), lidar-derived PBLH (dotted green), and PBLH based on measured θ (round red marker) are also included for comparison.

PBLH DA vs. T&q DA

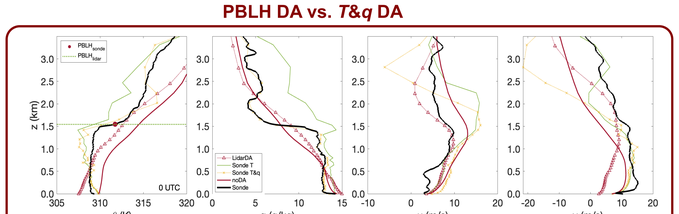


Fig. 9. Same as Fig. 8 but for comparison between Lidar PBLH DA with MP and the radiosonde measured T and q DA (solid green: Sonde T; solid yellow: Sonde T&q).

❖ Deterministic Forecast

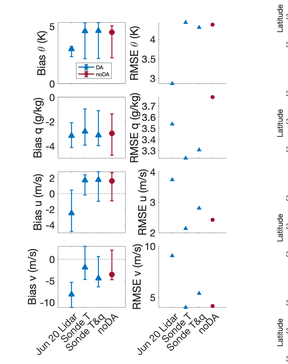
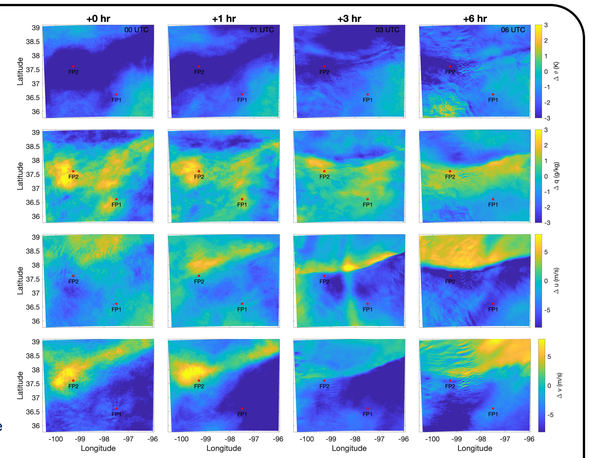


Fig. 11. Same as Fig. 10 but for the model forecast at 6 UTC (Fig. 13).



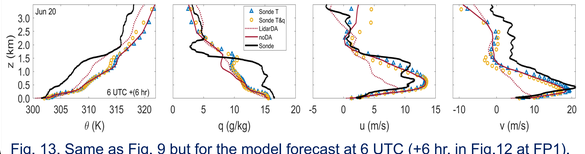


Fig. 13. Same as Fig. 9 but for the model forecast at 6 UTC (+6 hr. in Fig.12 at FP1).

Fig. 12. The spatial distribution of the θ, q, U, and V field differences between forecasts with DA and no-DA for June 20 case. The θ, q, U, and V field differences are the average over the lowest 20 model levels (~below 1.5 km), shown at 0, 1, 3, and 6 hours of the forecast.

❖ Impacts of Localization on the Analysis of PBLH and State Variables

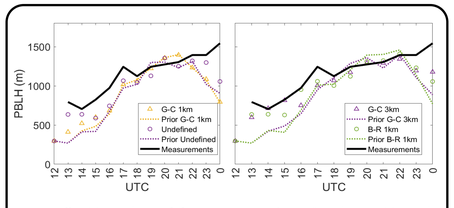


Fig. 6. Modeled PBLH during the Analysis-Model Advance cycles (assimilation window) at FP1. Dotted lines represent prior PBLH while unfilled markers denote posterior PBLH for various vertical localization types (see Fig. 4 a-c).

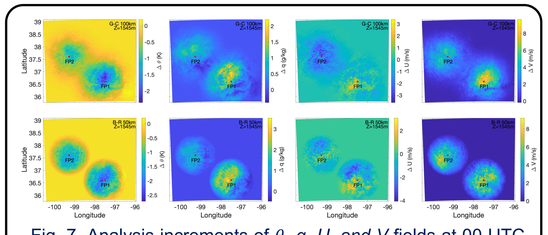


Fig. 7. Analysis increments of θ, q, U, and V fields at 00 UTC (Posterior-Prior fields interpolated at the height of lidar-measured PBLH) from two types of horizontal localization (see Fig. 4d).

Summary & Future Work

1. The utilization of multi-physics can improve DA performance.
2. The lidar PBLH DA and T&q profile DA can improve the analysis and forecast of θ (and slightly q). PBLH DA (T&q profile) appears to improve U (V) although also showing associated uncertainties.

Future work: Adding surface properties (soil moisture and temperature, etc.) to the updated state vector and investigate the impact (towards a coupled DA).

Acknowledgement

This work is supported by NASA Decadal Survey Incubation Grant 80NSSC22K1104 (NNH21ZDA001N-DSI) (Co-Is: A. Arellano/UA, B. Demoz/UMBC, J. Santanello/NASA GSFC, and W. Blumberg/NASA GSFC, Collaborators: J. Anderson/NCAR, A. Tangborn/NOAA).